Deriving Hydrometeor Mass from Simulated Images with Machine Learning

Kwo-Sen Kuo[1,2] and Robert S. Schrom[1,2]

1. NASA Goddard Space Flight Center, Greenbelt, Maryland, USA
2. Earth System Science Interdisciplinary Center, University of Maryland, College Park, Maryland, USA

Background

- Mass-dimensional relations, $m - D$ or $m(D)$, provide an important constraint to solid-phase precipitation retrievals and microphysics parameterizations.
- Most $m - D$ relations are expressed as a power law, $m(D) = aD^b$, between the particle's mass m and its maximum dimension D
  - *maximum dimension*: the largest distance between two points of/within the object
- The coefficients a and b are derived from *in situ* imaging probe measurements of ice particles at the Earth's surface or on aircraft platforms.
- The estimated maximum dimension, $\widetilde{D}$, is derived from projected maximum dimensions at a set of view directions, D_p^i, nearly always underestimating the true maximum dimension D for complex and non-convex aggregates, leading to biases in a and b.
- While it is challenging to estimate D, it is even more so to estimate mass, m.

Methodology

Simulating Probe Views

- Use > 14000 synthetic 3-D snow aggregates from the Kuo et al. (2016) database
  - We understand the limitations, for example, they are composed of monomers of the same "habit"
- Simulate a variety of probe configurations, each with a different number of camera views
- Each (i^{th}) camera view produces a 2-D projected maximum dimension, D_p^i
- The maximum dimension, D, is estimated as

$$\widetilde{D} = \max\left(D_p^i\right)$$

- We compare $\widetilde{D}$ with D to estimate biases.

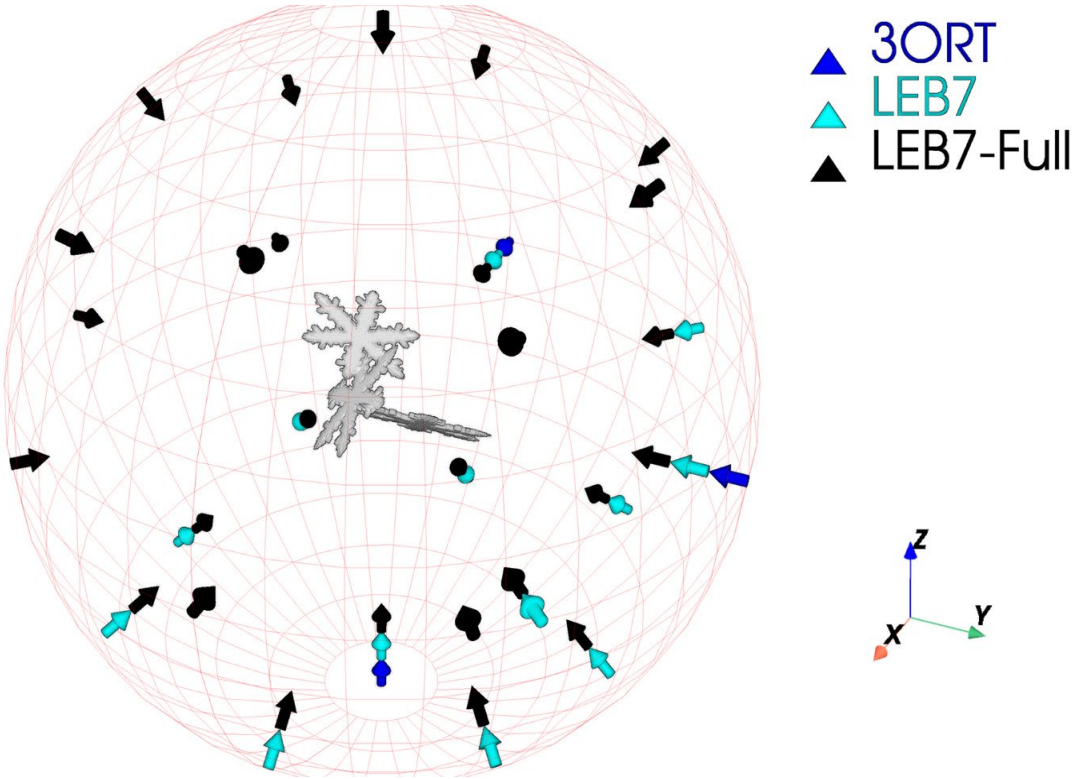

Probe View Simulations

- Single-vie
- Two-view
  horizonta
- Multi-ang
  horizonta
- Three-or
  cartesian
- Probes fo
  the azimu
  - Thes

View index	view zenith angle (°)	view azimuth angle (°)	probe(s)
1	90.0	0.0	SING,2DVD,MASC,3ORT,LEB7
1a	90.0	36.0	MASC
1b	90.0	72.0	MASC
2	90.0	90.0	2DVD,3ORT,LEB7
3	0.0	90.0	3ORT,LEB7
4	45.0	90.0	LEB7
5	45.0	-90.0	LEB7
6	45.0	0.0	LEB7
7	45.0	180.0	LEB7
8	90.0	45.0	LEB7
9	90.0	135.0	LEB7
10	54.7	45.0	LEB7
11	54.7	-45.0	LEB7
12	54.7	135.0	LEB7
13	54.7	-135.0	LEB7

vs in the

the

ree

that follow

Error Decreases with More Views

- *Unform Random Orientation*

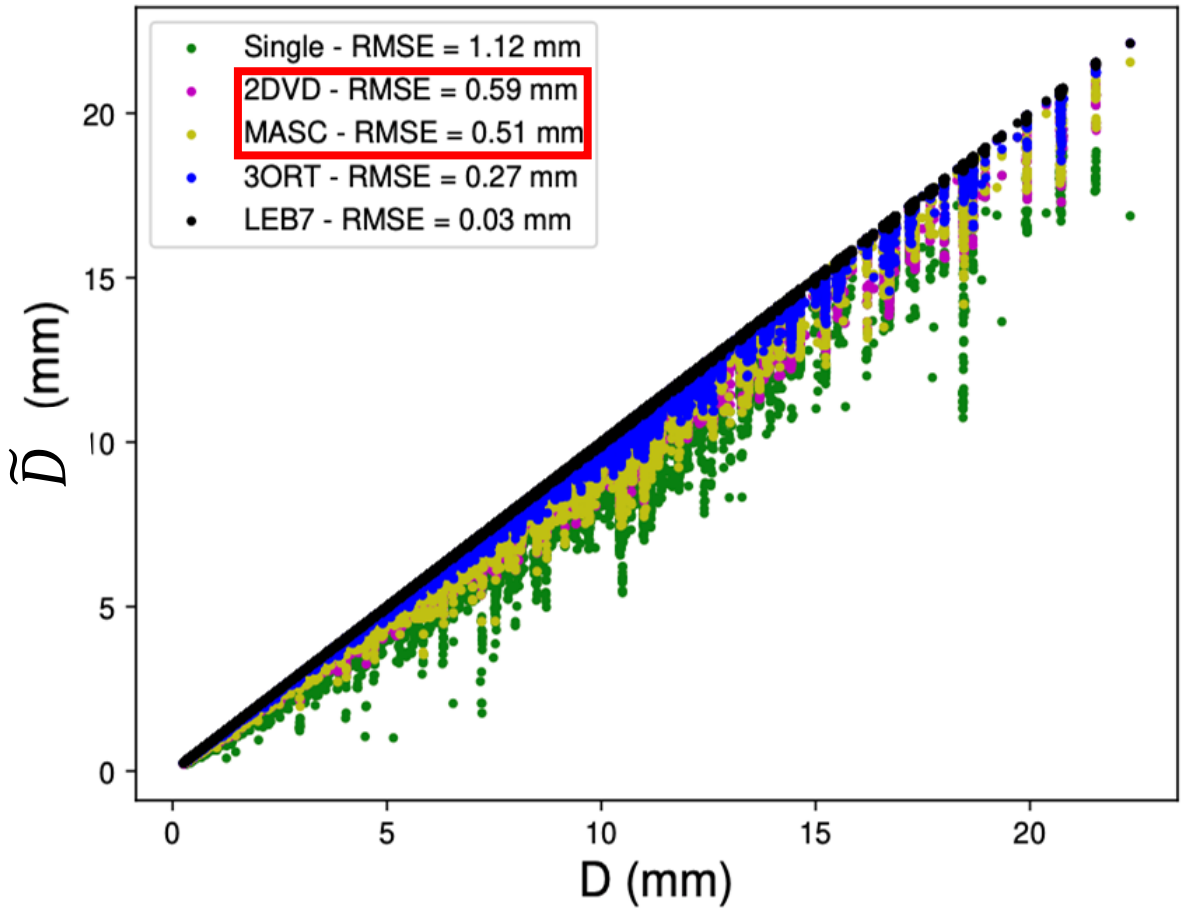

Orientation (In)dependence

Snowflakes fall with preferential orientations.

Orientation Distribution

- The previous slide shows biases for particles with uniformly ran
- Next, we examine azimuthally symmetric random orientation di
- We use a set of 770 orientations specified by the quadrature nc easy integration
- We use the Euler angles α and β to characterize the particle ori
  - ~~Since D_p is invariant to rotations of γ, the third Euler angle γ is ex~~
  - In addition, we assume α distribution is uniform, i.e., azimuthally
- The β angle follows a beta distribution: $f_i = \frac{1}{4\pi B(1,h)}\left(1+\frac{\cos\beta_i}{2}\right)^{h-1}$
  - The distribution of $\cos\beta$ is uniform, when $h = 1$
  - As h increases it becomes more horizontally aligned

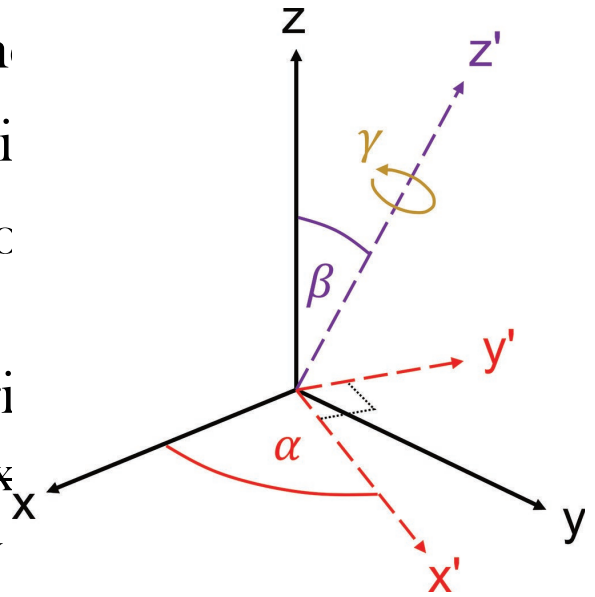

Important Notes

- Camera views at Lebedev-7 (LEB7) nodes are used to study orientation distribution
  - Its first 3 nodes correspond to SING, 2DVD, and 3ORT configurations
  - Camera view is added one by one following the order shown in the table
- There is a $\widetilde{D}_j^k$ for each orientation distribution (j) and each probe-view configuration (k), i.e., $\widetilde{D} \equiv \widetilde{D}(j,k)$. Thus, $m-D$ is contoured in the following plots.
- The literature reports many $m-D$ relations, we focus on two here
  - Mitchell et al. (1990) (**M90**), $m = \mathbf{0.006}D^{\mathbf{1.80}}$
  - Heymsfield et al. (2010) (**H10**), $m = \mathbf{0.077}D^{\mathbf{2.05}}$
  - Units: kilogram (kg) for m and meter (m) for D

Estimated vs *True* $m - D$ Coefficients

Estimated: $\tilde{a}, \tilde{b}$

- Extract aggregates with m and D that follow M90 and H10, assuming they apply to real D
- Use probe-derived $\tilde{D}$ corresponding to D of the extracted to find $\tilde{a}$ and $\tilde{b}$

True: $\acute{a}, \acute{b}$

- Extract particles with m and D corresponding to $\tilde{D}$ that follow M90 and H10
- Use extracted m and D to find $\acute{a}$ and $\acute{b}$

Estimated coefficients: $\tilde{a}$ and $\tilde{b}$

- $\tilde{a}$ color filled; $\tilde{b}$ cyan contour
- The *estimated* coefficients have minimal dependence on the degree of horizontal alignment.
- The difference between estimates and truths decreases rapidly as the number of probe views increases.
- The errors decrease more rapidly for the M90 coefficients than for the H10 coefficients.

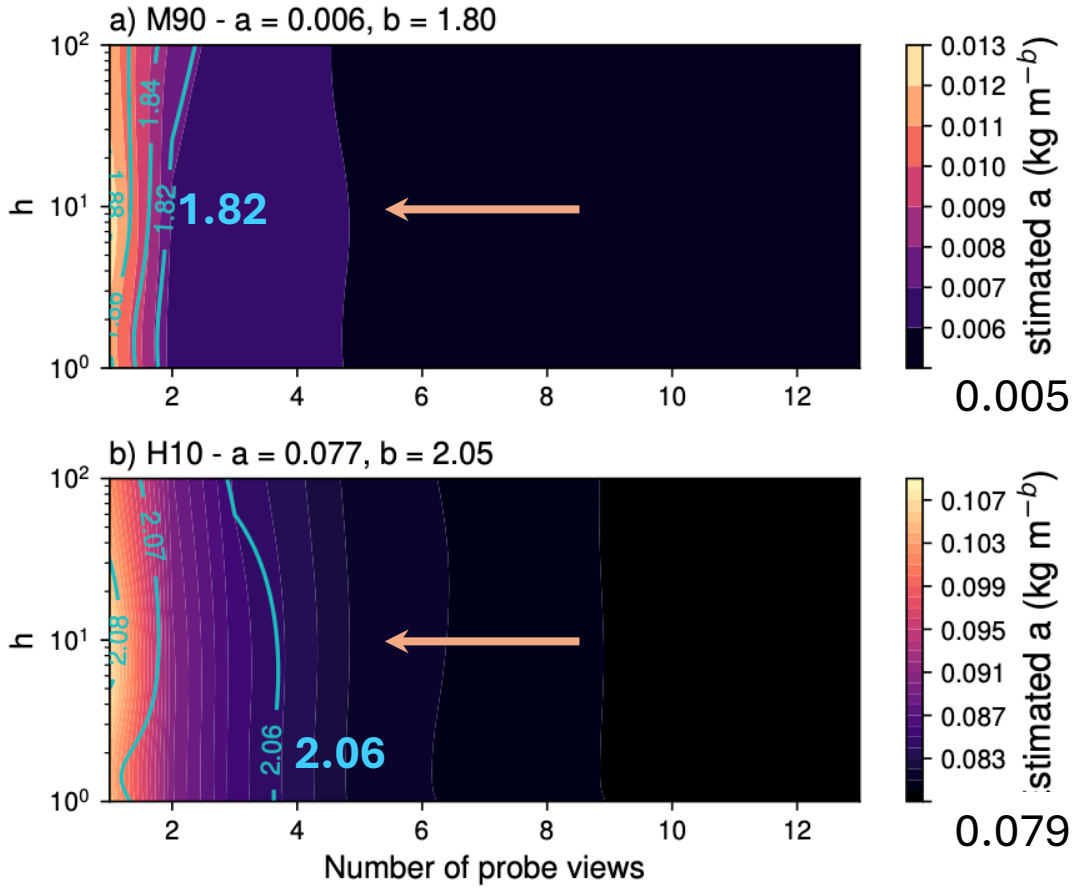

True Coefficients: *á* and *b́*

- *á* color filled; *b́* cyan contour
- The *true* coefficients have minimal dependence on the degree of horizontal alignment.
- The difference between estimates and truths decreases rapidly as the number of probe views increases.
- The errors decrease more rapidly for the M90 coefficients than for the H10 coefficients.

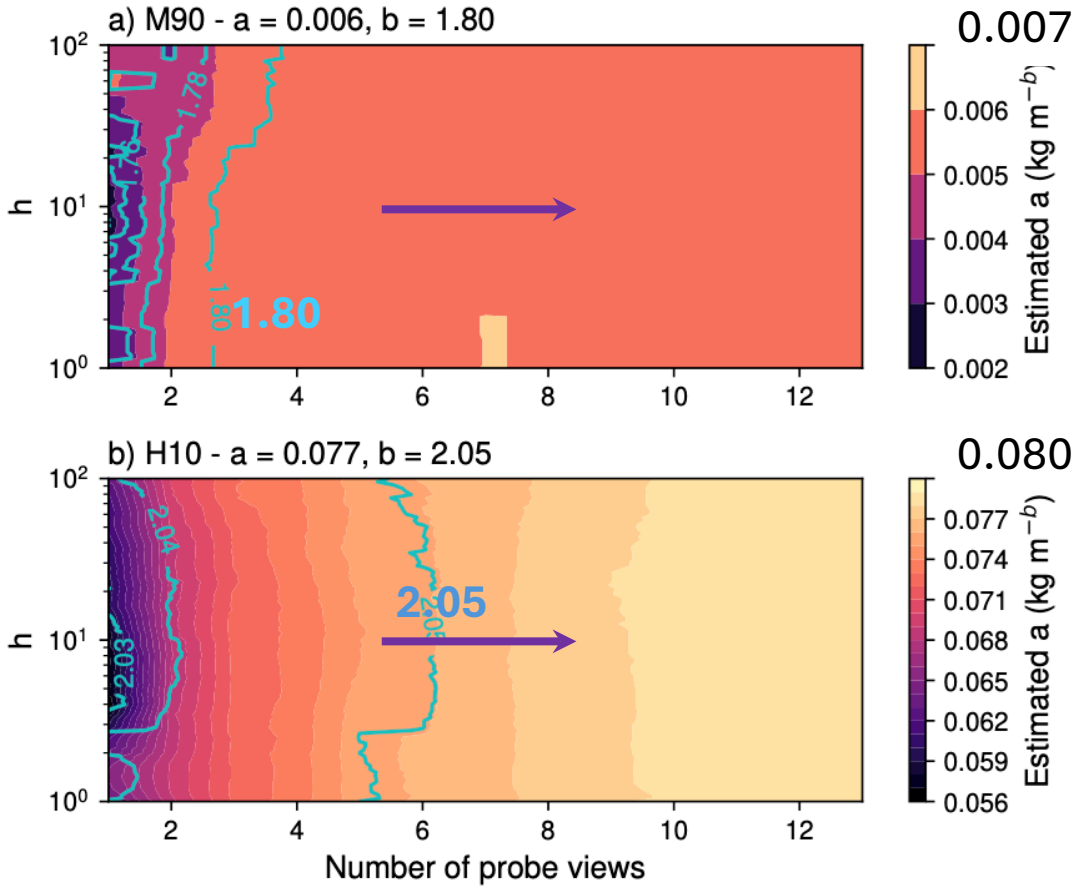

$m - D$ Impact on Ice Water Content

Impact on Ice Water Content

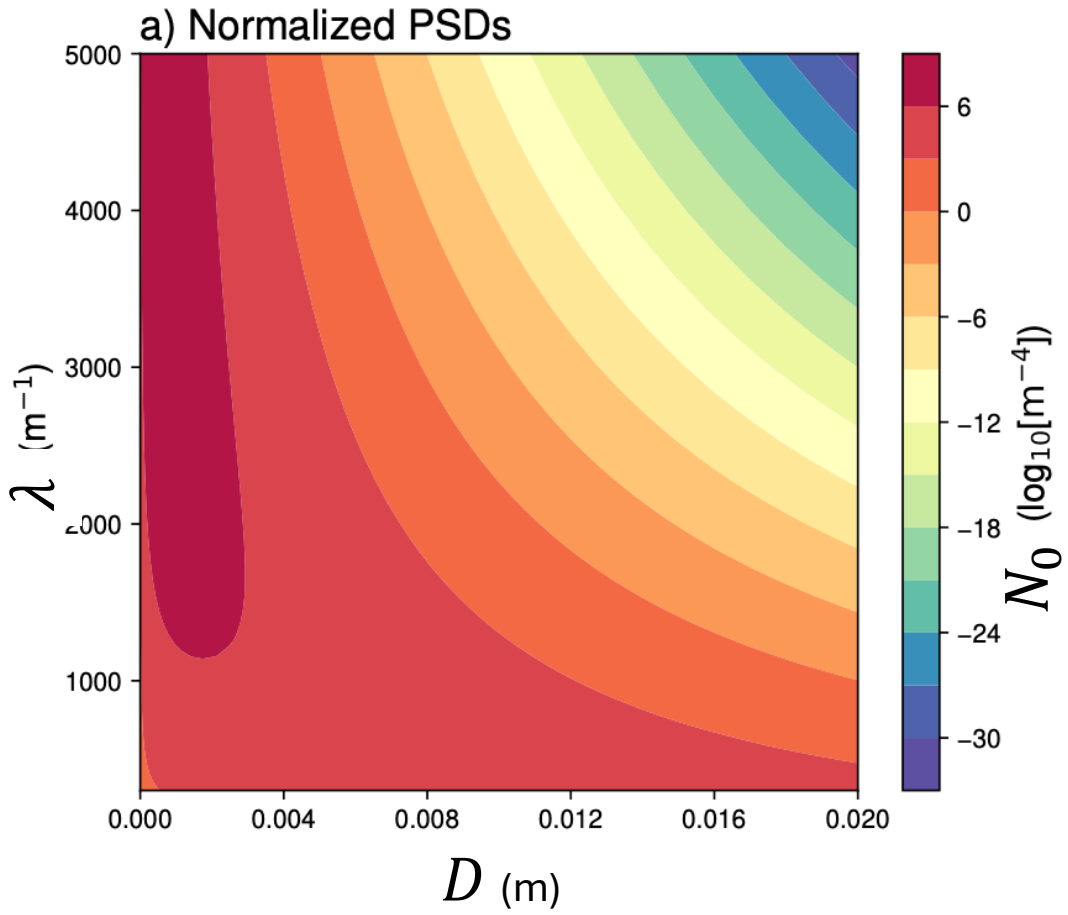

- Since $m - D$ is insensitive to orientation, uniform random distribution is used
- Simulate a range of particle size distributions (PSDs) normalized to ice water content (IWC) of 1 g m^{-3}.
  - Gamma distribution with $\mu = 2$

$$N(D) = N_0 D^{\mu} e^{-\lambda D}$$

- Calculate the IWC using the *estimated* $m - D$ relation coefficients $\tilde{a}$ and $\tilde{b}$ associated with each LEB7 probe configuration for the M90 and H10 coefficients.

Biases in $m - D$ Produce Large IWC Errors

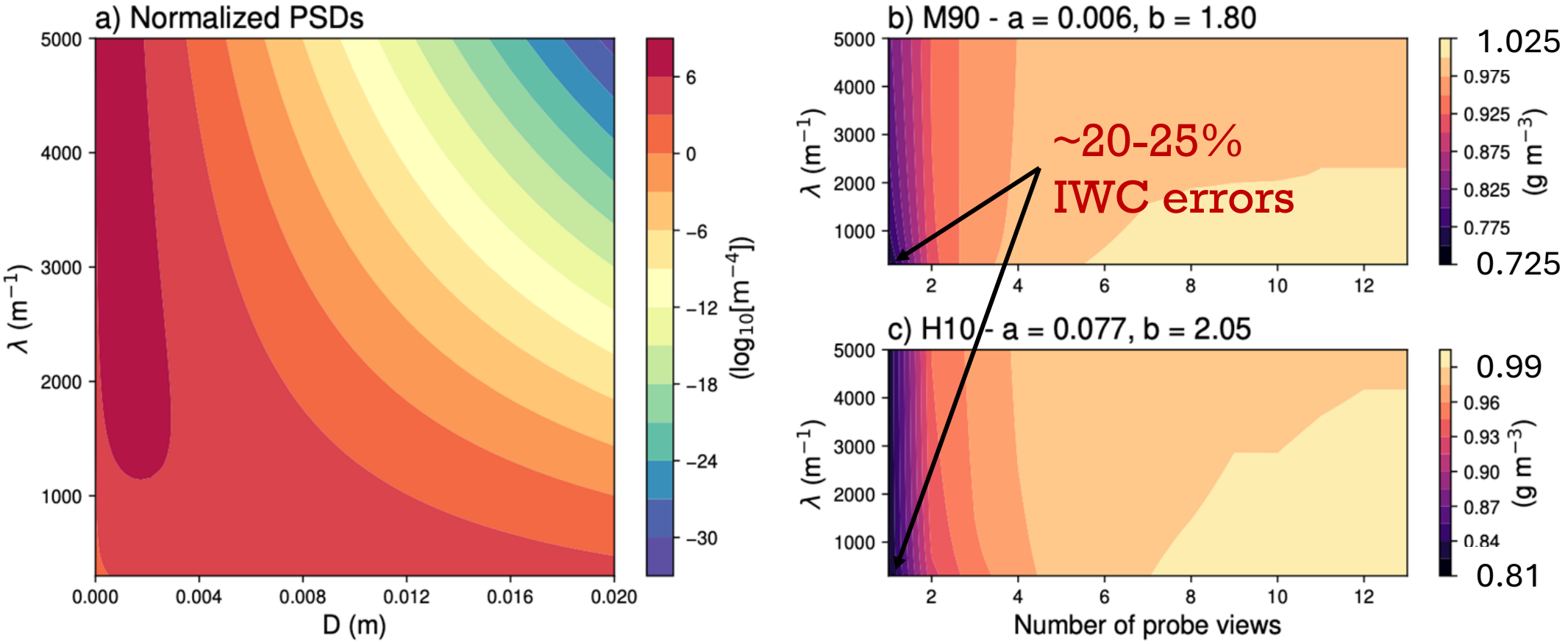

Multiparameter Estimation with Machine Learning (ML)

A preliminary feasibility investigation

Multiparameter Prediction with CNN

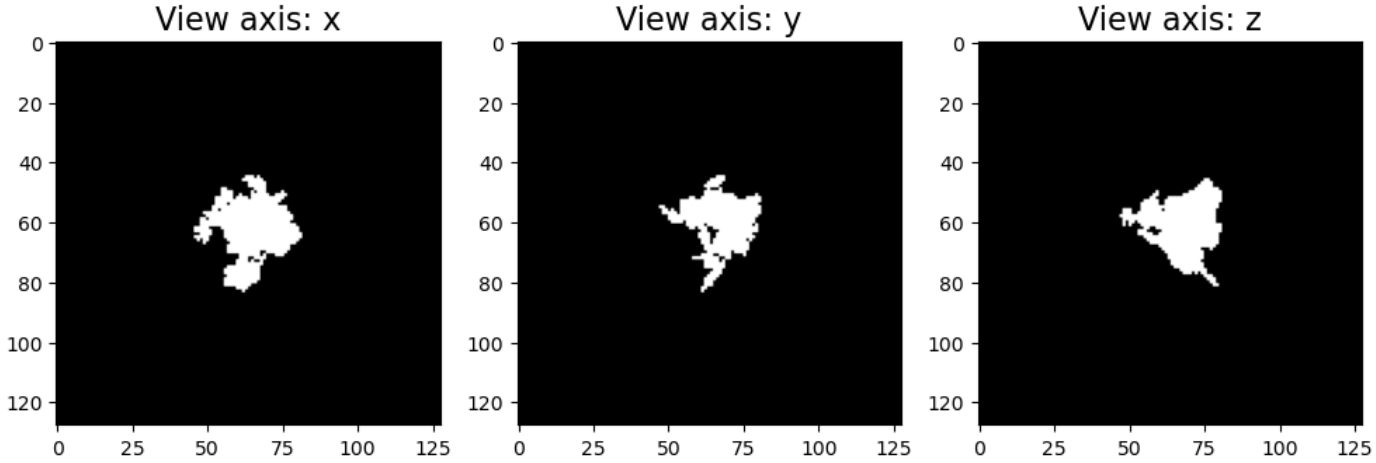

- Generate synthetic projected images of 128×128 pixels from 3 orthogonal view directions along *x*, *y*, and *z* axes for 5200 snow aggregates from the Kuo et al. (2016) database.
- Feed 80% of the image data as three channels to train a convolutional neural network (CNN) with TensorFlow. Use 20% for testing.
  - 5 alternating convolution and max pooling layers are used,
  - The output is reduced to a scalar value (either maximum dimension, number of dipoles, or effective density).
  - There are 2555 training parameters.

CNN Prediction:

D

- The CNN-predicted D vs. true values fall close to the one-to-one line.
- The CNN-predicted D overestimates for the smallest particles ($D < 2$ mm).

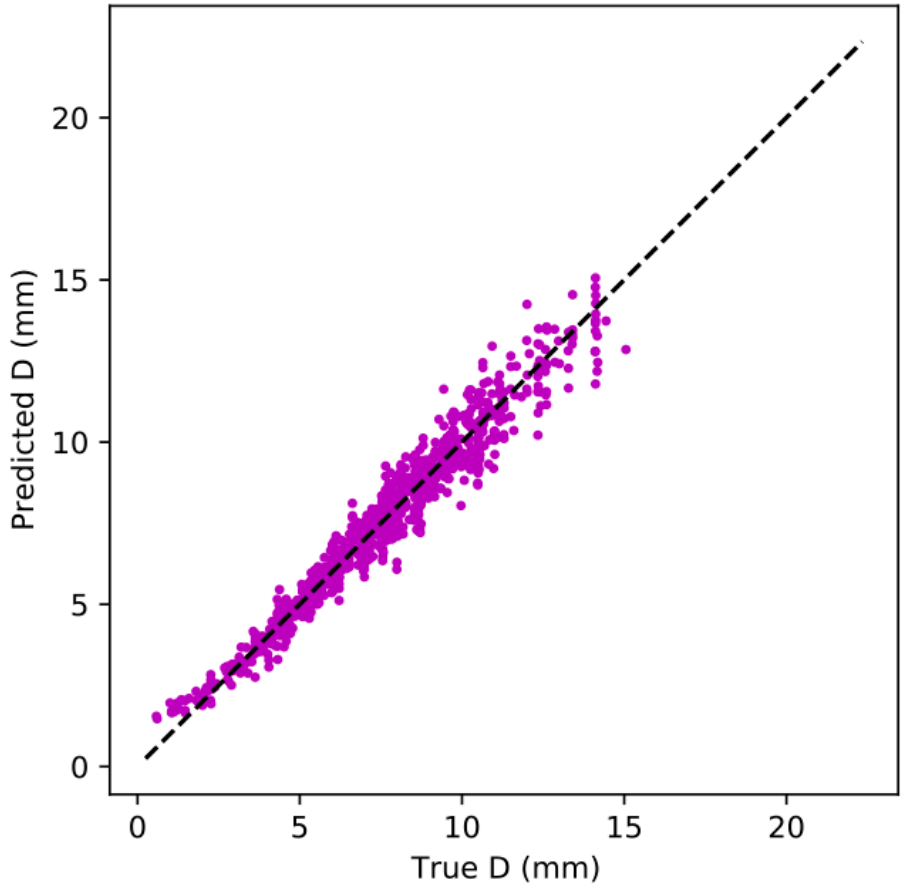

CNN Prediction:

$$m$$

- The number of dipoles is proportional to particle volume and mass.
- The error in the CNN-predicted values increases as the number of dipole increases (in this configuration of 3 orthogonal views).

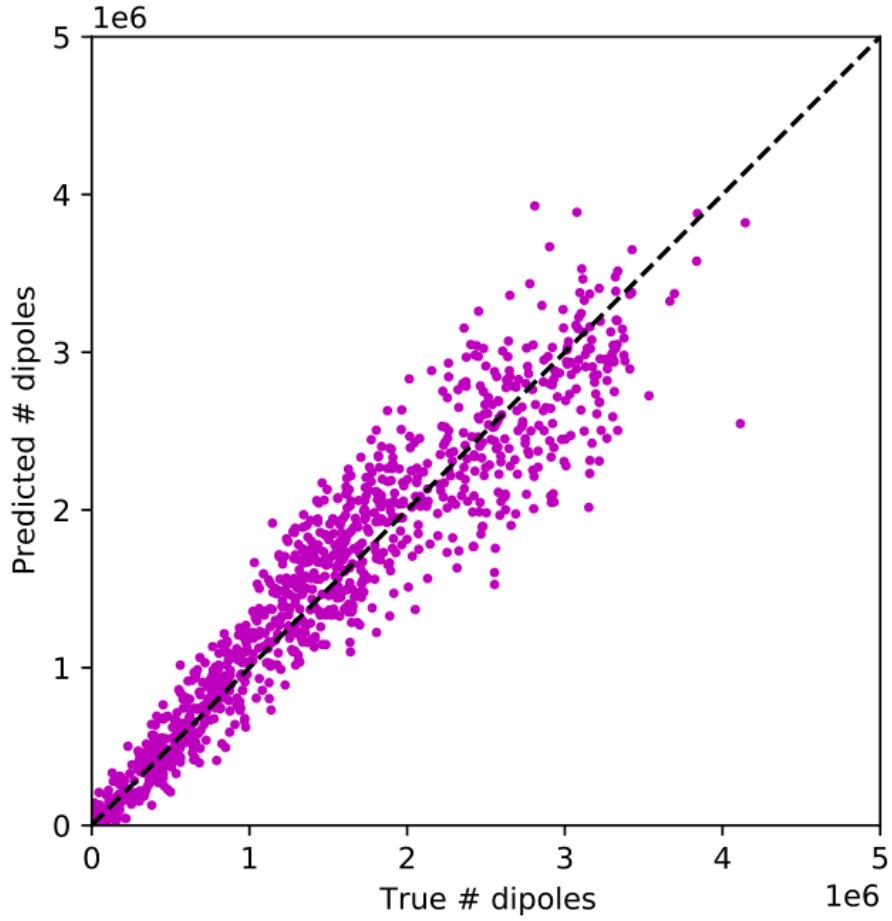

CNN Prediction:

ρ_e

- Effective density, $\rho_{e(ff)}$, defined as the particle mass divided by its convex-hull volume.
- Most effective density values are < 200 kg m^{-3};
- CNN-predicted values versus true values fall close to the one-to-one line.

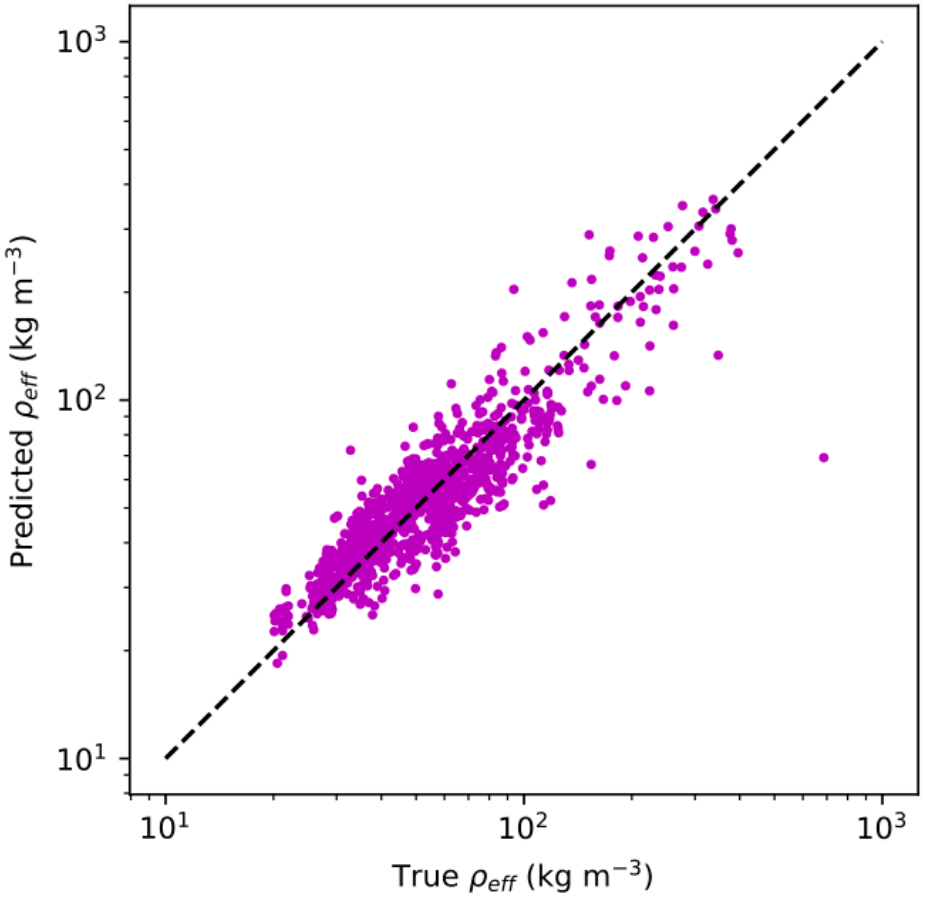

Conclusions

- The number of less correlated probe views determines the accuracy of maximum dimension estimates from imaging-probe instruments.
- Using > 3 probe views in LEB7 configurations greatly reduces the errors in $\widetilde{D}$ and, thus, the biases in the resulting $m - D$ relation coefficients and derived ice water contents.
- Retrieval uncertainties using $m - D$ relations derived from 1-2 views must be reassessed.
- Machine learning techniques show promise for estimating multiple particle geometric properties simultaneously, especially if more independent views are provided.
  - *e.g.*, the instrument developed by Bringi and Notaros has 7 camera views.

References

Garrett, T. J., Fallgatter, C., Shkurko, K., & Howlett, D. (2012). Fall speed measurement and high-resolution multi-angle photography of hydrometeors in free fall. Atm. Meas. Tech., 5 , 2625--2633.

Heymsfield, A. J., Schmitt, C., Bansemer, A., & Twohy, C. H. (2010). Improved representation of ice particle masses based on observations in natural clouds. J. Atmos. Sci., 67 , 3303–3318.

Kruger, A., & Krajewski, W. F. (2002). Two-dimensional video disdrometer: A description. J. Atmos. Oceanic Technol., 19 , 602–617.

Kuo, K., Olson, W. S., Johnson, B. T., Grecu, M., Tian, L., Clune, T. L., Meneghini, R. (2016). The microwave radiative properties of falling snow derived from nonspherical ice particle models. Part I: An extensive database of simulated pristine crystals and aggregate particles, and their scattering properties. J. Appl. Meteor. Climatol., 56 , 691–708.

Mitchell, D. L., Zhang, R., & Pitter, R. L. (1990). Mass-dimensional relationships for ice particles and the influence of riming on snowfall rates. J. Appl. Meteor., 29 , 153–1723.

Thank you!

Acknowledgment: We are grateful for the support of NASA Precipitation Measurement Missions (PMM).